Applied Catalysis B: Environmental 220 (2018) 506–511

Contents lists available at ScienceDirect

Applied Catalysis B: Environmental

journal homepage: www.elsevier.com/locate/apcatb

In-situ characterization by Near-Ambient Pressure XPS of the catalytically active phase of Pt/Al_2O_3 during NO and CO oxidation

Susanna L. Bergman[a,g,1], Jonas Granestrand[b,1], Yu Tang[c], Rodrigo Suárez París[d], Marita Nilsson[e], Franklin Feng Tao[c], Chunhua Tang[f], Stephen J. Pennycook[f], Lars J. Pettersson[b], Steven L. Bernasek[a,g,*]

[a] Department of Chemistry, Princeton University, Princeton, NJ, 08544, USA
[b] Department of Chemical Engineering, KTH Royal Institute of Technology, Stockholm, SE-10044, Sweden
[c] Department of Chemical and Petroleum Engineering and Department of Chemistry, University of Kansas, Lawrence, KS, 66045, USA
[d] Materials Technology, Scania CV AB, Södertälje, SE-15187, Sweden
[e] Catalytic Converter and Particulate Filter Performance, Scania CV AB, Södertälje, SE-15187, Sweden
[f] Department of Materials Science and Engineering, National University of Singapore, 117608, Singapore
[g] Science Division, Yale-NUS College, Singapore, 138527, Singapore

ARTICLE INFO

Keywords:
Diesel oxidation catalyst
In-situ
NAP-XPS
Active catalytic
Phase
Platinum

ABSTRACT

This study concerns near ambient pressure X-ray photoelectron spectroscopy (NAP-XPS) studies of a Pt/Al_2O_3 diesel oxidation catalyst used in exhaust aftertreatment. We apply the technique to an industrial-grade porous catalyst, thus bridging both the pressure and materials gap, and probe the shift in binding energy of Pt 4d under different atmospheres. We observe that oxidizing atmospheres induce a shift in binding energy, corresponding to changes in Pt oxidation state, especially pronounced under an atmosphere of NO and O_2. Such changes in Pt oxidation state have previously been linked to dynamic changes in NO oxidation activity.

1. Introduction

Emission standards legislation limits the amounts of CO, hydrocarbons, nitrogen oxides (NOx), and particulate matter that can be emitted from vehicles [1]. For heavy-duty diesel vehicles, emission standards are typically adhered to by using a combination of diesel oxidation catalysts (DOC) [2], diesel particulate filters [3], selective catalytic reduction (SCR) catalysts [4] and ammonia slip catalysts [4]. Fig. 1 shows Scania's heavy-duty Euro 6 aftertreatment system as an example. The DOC is frequently placed first in the exhaust after-treatment system and is of key importance for the overall effectiveness [2]. An important function of the oxidation catalyst is to oxidize NO, as NO_2 improves soot oxidation over the particulate filter and enables fast reduction of NO_x over the SCR; in addition, the DOC oxidizes CO and unburned hydrocarbons to carbon dioxide and water [2].

During reaction, catalyst surfaces are exposed to a gas stream with a complex composition, so characterization before and after the reaction may not reflect significant changes of the surface chemistry that take place during reaction. As most catalytic surfaces consist of metallic nanoparticles or oxides and, thus, are sensitive to oxidizing or reducing agents, it is highly probable that many catalytic surfaces will be different under reaction atmospheres, as compared to before or after a reaction takes place. For example, it has previously been shown that both Pt [5] and Cu [6] nanoparticles exhibit reversible structural changes under working conditions. As this has major implications for aftertreatment catalysts, an in situ or operando approach is necessary when characterizing these materials. Near-Ambient Pressure X-ray Photoelectron Spectroscopy (NAP-XPS) allows detailed X-ray photoelectron characterization of surfaces in the presence of reactants [7–10], and is therefore a promising tool for studying changes in surfaces during reaction. Of interest specifically for researchers in the field of diesel exhaust aftertreatment catalysis, NAP-XPS has previously been used to study CO oxidation on Pt(110) surfaces [11], on stepped (557) and (332) platinum surfaces [5], as well as on Pd(110) [12] Pd(100)

Abbreviations: ASC, ammonia slip catalyst; B.E., binding energy; DOC, diesel oxidation catalyst; EDS, Energy Dispersive Spectroscopy; EGR, Exhaust Gas Recirculation; GC, gas chromatograph; HAADF, high-angle annular dark-field; ICP-OES, inductively coupled plasma-optical emission spectroscopy; MS, mass spectrometer; NAP-XPS, Near-Ambient Pressure X-ray Photoelectron Spectroscopy; RGA, residual gas analyzer; SCR, selective catalytic reduction; STEM, Scanning Transmission Electron Microscopy; UHV, ultra-high vacuum; VGT, Variable-Geometry Turbocharger; XAS, X-Ray Absorption Spectroscopy

* Corresponding author at: Department of Chemistry, Princeton University, Princeton, NJ, 08544, USA.
E-mail address: steven.bernasek@yale-nus.edu.sg (S.L. Bernasek).
[1] These authors contributed equally.

http://dx.doi.org/10.1016/j.apcatb.2017.08.047
Received 2 June 2017; Received in revised form 8 August 2017; Accepted 14 August 2017
Available online 24 August 2017
0926-3373/

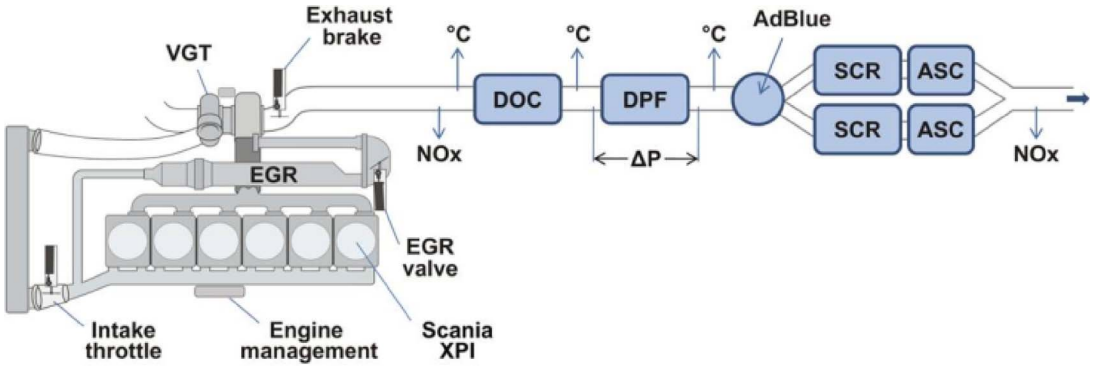

Fig. 1. Scania Euro 6 system including after-treatment. VGT – Variable-Geometry Turbocharger; EGR – Exhaust Gas Recirculation; XPI – Extra High-Pressure Injection; DOC – Diesel Oxidation Catalyst; DPF – Diesel Particulate Filter; ΔP – Pressure Drop; SCR – Selective Catalytic Reduction; ASC – Ammonia Slip Catalyst [published by kind permission of Scania CV AB].

[13], and Pd(111) [14] surfaces. In this study, we apply the technique to probe changes in the oxidation state of catalytically active Pt on supported, porous Pt/Al_2O_3 catalysts.

An interesting property of the NO oxidation reaction on supported platinum catalysts is that it exhibits reverse temperature hysteresis. While many other catalytic oxidation reactions are more active on cool-down than on heat-up, NO oxidation exhibits the opposite behavior [15]. The catalyst appears to be reversibly deactivated at high temperatures. Previous studies [16,17] had indicated that NO oxidation activity decreases as a consequence of formation of platinum oxides on the catalyst surface. Earlier XPS studies, following (ex-situ) [17] and during (in-situ) [18] exposure to nitrogen oxides had shown that NO_2 gives a more oxidized Pt surface than in UHV or upon treatment with O_2. This is indicated by the binding energy of the Pt 4f peak [17] or the Pt $4p_{3/2}$ to O 1s peak intensity ratio [18], respectively. Therefore, it was concluded that the reduced NO oxidation activity of Pt on cool-down was due to oxidation of the Pt surface by NO_2 formed in the reaction at higher temperatures. The link between transient changes in Pt oxidation state and NO oxidation activity was later further explored and strengthened by in-situ X-Ray Absorption Spectroscopy (XAS) studies [19].

Previous work has investigated CO oxidation by O_2 on platinum under a variety of conditions. Particularly relevant here is an earlier study of CO oxidation on the Pt(110) surface using high pressure XPS at a synchrotron facility [20]. In this study no firm evidence for surface Pt oxide formation was seen for O_2/CO ratios ≪10, and at surface temperatures between 100 and 150 °C, although a high energy shoulder in the Pt 4f spectra was observed at the high temperature end of this range. In a study of CO oxidation over Pt particles supported on Al_2O_3, Manasilp and Gulari [21] found that for 1–1 CO/O_2 ratios, and temperatures ≪200 °C, CO conversion to CO_2 was nearly 100%. They found that the presence of water in the reactant stream increased the catalyst activity under these conditions.

A number of groups have also examined NO oxidation over supported Pt catalysts, relevant to the study reported here. Experimental evidence for a reverse hysteresis in NO oxidation [22] was obtained by kinetic studies which suggest that Pt oxides formed at intermediate temperatures (200–300 °C) in the NO + O_2 stream are reduced by NO at lower catalyst temperatures (≪200 °C), reactivating the less active Pt oxide material. At temperatures greater than 300 °C, the Pt oxide starts to become unstable and begins to decompose, leaving Pt metal particles. XPS studies confirmed this idea [23], showing that Pt oxide does form on the catalyst surface in these intermediate temperatures, as evidenced by the Pt 4f and 4d binding energies following exposure to NO/air or NO_2/air streams at 300 °C and allowed to cool in the stream. This study also showed an interesting particle size effect, with 7 nm average size Pt particles exhibiting four times the activity of 2.4 nm average size particles for the production of NO_2 from NO. Boubnov et al. [19] also observed a particle size effect on NO oxidation activity. Their XAFS results suggested that this was due to the effect of particle size on Pt oxide formation.

Kinetic modeling studies of the NO oxidation over supported Pt catalysts were also carried out [24]. These studies developed a kinetic model consistent with the hysteresis described above, and supported the idea that Pt oxides are formed at intermediate temperatures in the oxidizing reactant stream. These oxides are reduced by NO at lower temperatures, and the production of NO_2 at higher temperatures leads to further Pt oxide formation, which deactivates the catalyst at higher temperatures. Further experimental kinetic studies [25] showed that steady state is not reached during NO oxidation, and that the Pt/Al_2O_3 catalyst deactivates over time in contact with the NO_2 product of the NO oxidation reactant. These workers suggested the formation of Pt oxides or Pt with chemisorbed oxygen on the deactivated surface as the reason for the deactivation, although no spectroscopic evidence for oxide formation was provided.

The discussion above highlights the importance of characterizing the catalyst surface in the presence of reactants and products present during reaction conditions. As described above, this has successfully been done before using in-situ XAS and in-situ XPS at synchrotron light sources [18,19]. Synchrotron sources may be unavailable or prohibitively expensive for commercial use by catalyst manufacturers and vehicle manufacturers. In this study, we demonstrate that using a lab-scale NAP-XPS instrument can make it possible to probe changes in oxidation state of the catalytic phase of industrial grade, porous Pt/Al_2O_3 catalysts under exposure to gas phase reactants that model exhaust conditions.

2. Experimental methods

Catalysts were synthesized by a two-step incipient wetness impregnation, using a water solution of $Pt(NO_3)_4$ and γ-Al_2O_3 support, followed by drying at 110 °C and calcining for 4 h at 500 °C. The platinum loading was determined, by ICP-OES, to be 1.1 wt-%.

The laboratory-based NAP-XPS systems used operated according to the principles reported by Nguyen and Tao [26]. A schematic representation is given in Fig. 2.

Two independent gas lines were used to control the partial pressures independently of each other. The gas streams from both lines were mixed and allowed to flow through the reaction cell. Two sets of experiments were carried out, using two different NAP-XPS instruments, in order to judge reproducibility. Samples were initially outgassed at 700 K in UHV prior to measurements under controlled atmospheres. Prior to each experiment, the catalysts were reduced in flowing hydrogen at 500 K. In the first series of experiments, Al 2p and Pt 4d spectra were acquired in UHV and in O_2, NO, CO, NO + O_2 and CO + O_2 atmospheres. The partial pressure of each component was 1 Torr,

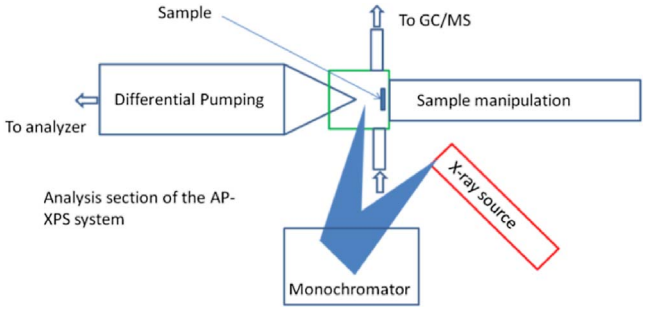

Fig. 2. Schematic of the NAP–XPS setup used for in-situ characterization.

giving a total pressure of 2 Torr for the mixed atmospheres. During spectrum acquisition, the temperature in the gas cell was 500 K. Additionally, spectra were acquired at 400 K in UHV, O_2 and NO atmospheres. The gases used had a purity of 99.99% or higher. A monochromated Al K-alpha X-ray source was used. A residual gas analyzer (RGA) quadrupole mass spectrometer was used to monitor the composition of gases exiting the in-situ cell. All binding energies presented are corrected for sample charging by referencing against the literature value of Al 2p at 74.5 eV. The spectrometer is calibrated to the Au 4f peak position. A Shirley background and standard restriction parameters were used for peak fitting. No differential charging was observed.

In diesel vehicle exhaust, the concentration of O_2 is orders of magnitudes higher than the concentrations of CO and NO. To more accurately mimic these conditions, a second set of mixed atmosphere experiments was performed, where pressures were chosen to give partial pressures of O_2 100 times higher than the partial pressure of CO and NO. For CO and O_2, bottles of high purity gas were used, while for NO, a gas mixture (100 ppm NO in balance N_2) was used. In this set of experiments, Al 2p and Pt 4d spectra were acquired in each atmosphere. A Mg-Al twin anode X-ray source was used. The sample was reduced for 30 min in H_2 with the sample at 500 K before each new atmosphere was introduced to ensure a similar degree of reduction at the start of each experiment.

For Scanning Transmission Electron Microscopy (STEM) examination of the catalyst, the as-prepared catalyst powder was dispersed in ethanol, deposited on a Cu mesh with lacey carbon film, and examined using a JEOL JEM-ARM200F with ASCOR corrector. High Angle Annular Dark Field (HAADF) [27] imaging was carried out at 200 keV acceleration voltage. Energy Dispersive Spectroscopy (EDS) (Oxford X-Max^N 100TLE) was used to provide elemental mapping of the sample, monitoring Pt, Al, and O.

The average Pt particle size was estimated by CO chemisorption. After evacuation, samples were reduced by hydrogen for 2 h at 400 °C

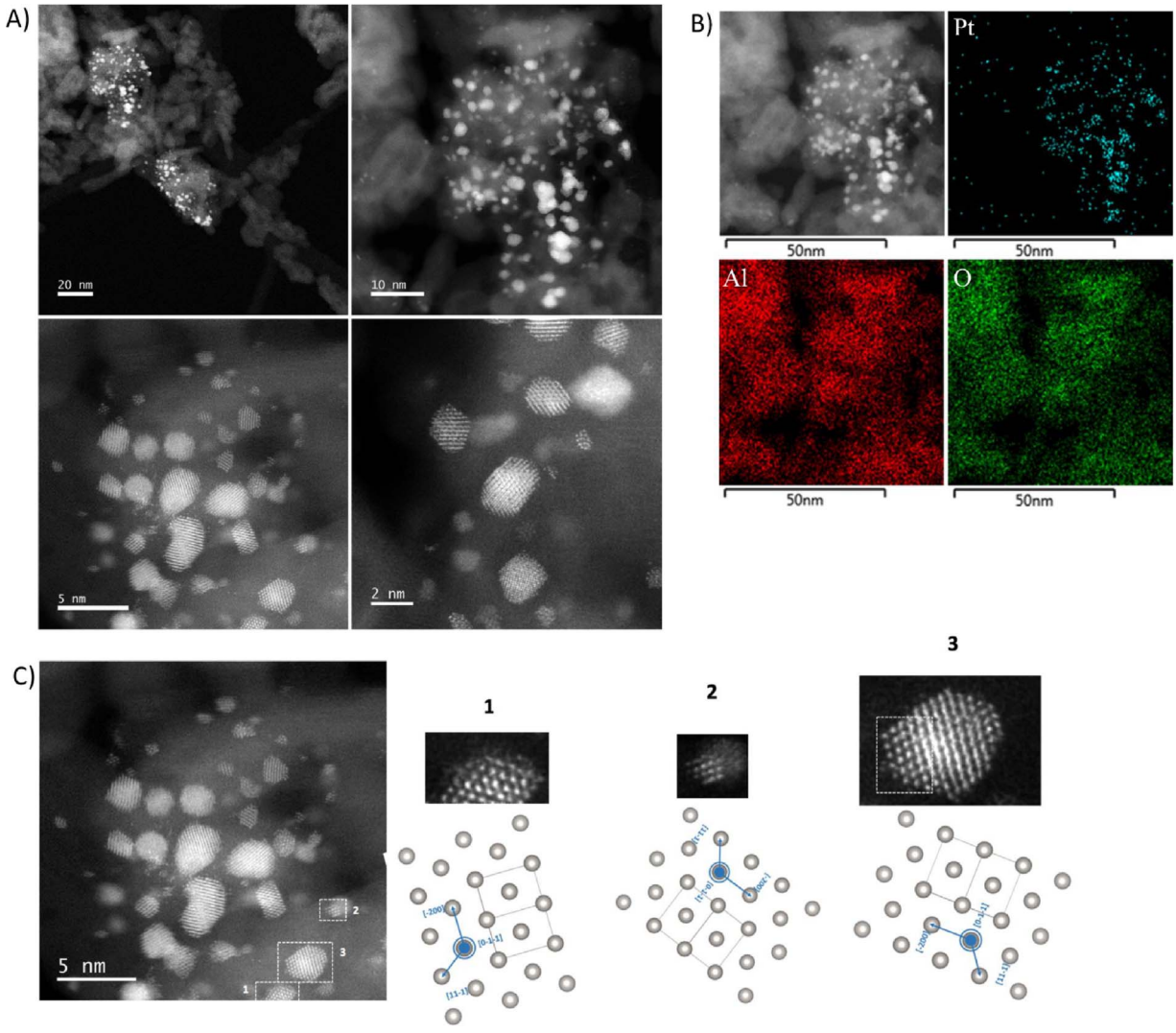

Fig. 3. A) STEM images of as prepared catalyst at various magnifications, showing Pt particle sizes in the range of 2–5 nm B) EDS mapping of Pt, Al, and O, showing that Pt is not collocated with O C) Zone axis analysis of selected particles, showing Pt particle crystal orientation.

followed by analysis using a double isotherm method. After the first acquisition, samples were evacuated to remove physisorbed CO before a second isotherm was acquired, which then only corresponds to chemisorbed CO. The amount of chemisorbed CO was determined by extrapolating the linear portion of the isotherms to zero pressure and taking the difference between this value for the two isotherms. The dispersion was calculated by assuming an adsorption stoichiometry of CO on platinum of 1:1 (corresponding to linearly bonded CO) and comparing the amount of chemisorbed CO to the total number of Pt atoms in the sample. The average Pt particle size (d) was finally calculated from the percent dispersion (%D) using Eq. (1) [28], below.

$$d = \frac{108\%}{D} \quad (1)(1)$$

3. Results and discussion

3.1. TEM and chemisorption

According to CO chemisorption, the Pt/Al_2O_3 catalyst had a dispersion of 62%, corresponding to an average particle size of 2 nm. This is confirmed by the STEM images of the catalyst shown in Fig. 3. Pt particles in the sample are predominantly 2–3 nm in size, with a few particles reaching up to 5 nm in dimension. EDS mapping confirms that these nanoparticles are predominantly metallic Pt, with no evidence of oxygen localized with the Pt particles. Examination of the crystal plane spacing in the nanoparticles is also consistent with their identification as metallic Pt. Mostly (200) planes are seen, with spacing corresponding to metallic Pt (JCPDS #04-0802). The particles generally appear cubic in form, which would expose (100) surface planes. Close examination of the zone axis of several visible particles suggest that cubo-octahedral particles predominate.

3.2. UHV-XPS and NAP-XPS

The binding energy (B.E.) of the Pt $4d_{5/2}$ peak under varying experimental conditions is given in Table 1. The trend in peak shift is further illustrated in Fig. 4. The largest difference is exhibited under a reaction atmosphere of NO + O_2 (1.3 eV compared to UHV conditions). This value corresponds to a significant oxidation of the Pt and is in agreement with earlier studies where similar shifts were recorded after pretreatment in NO_2 and O_2 [17].

The reaction conditions can be divided into three groups with regards to how the binding energy of Pt $4d_{5/2}$ is affected. The first group has the Pt $4d_{5/2}$ peak at around 314.5 eV and contains the UHV and CO atmospheres. These atmospheres lack any oxidizing component and Pt is expected to be in a fully reduced, metallic state. For the second group, the binding energy of Pt $4d_{5/2}$ appears around 315.5 eV. The O_2, NO and CO + O_2 atmospheres can all be found here. The binding energy of Pt $4d_{5/2}$ is shifted considerably higher, indicating an increase of Pt oxidation state induced by the presence of O_2 or NO. Finally, when the sample was subjected to a NO + O_2 atmosphere, the Pt $4d_{5/2}$ binding energy shows further oxidation, with a shift to around 315.9 eV. A residual gas analyzer detected the presence of NO_2 (the product of the NO oxidation reaction) in these experiments. It appears that the presence of NO_2 causes an even greater oxidation of Pt compared to the other atmospheres. Both CO + O_2 exposure and NO + O_2 exposure result in an increase in oxidation state of the Pt greater than observed for CO, O_2, or NO individually. While the catalytic reactions forming CO_2 or NO_2 respectively, in the mixed gas exposures, are both examples of coverage sensitive reactivity, [18,29] NO_2 is an efficient O atom donor, while CO_2 is not so readily dissociated on Pt, resulting in more extensive oxide formation in the mixed NO + O_2 gas stream.

Table 1
B.E. of Pt $4d_{5/2}$ as a function of reaction atmosphere composition and temperature.

Atmosphere	Pressure (mbar)	Temperature (K)	XPS system	Pt $4d_{5/2}$ B.E.
UHV	10^{-9}	400	1	314.3
UHV	10^{-9}	500	1	314.6
UHV	10^{-9}	500	2	314.5
CO	1.3	500	1	314.3
O_2	1.3	400	1	314.9
O_2	1.3	500	1	315.3
NO	1.3	400	1	315.2
NO	1.3	500	1	315.2
CO + O_2	1.3 + 1.3	500	1	315.4
CO + O_2	$10^{-4} + 10^{-2}$	500	2	315.6
NO + O_2	1.3 + 1.3	500	1	315.9
NO + O_2	$10^{-4} + 10^{-2}$	500	2	315.9

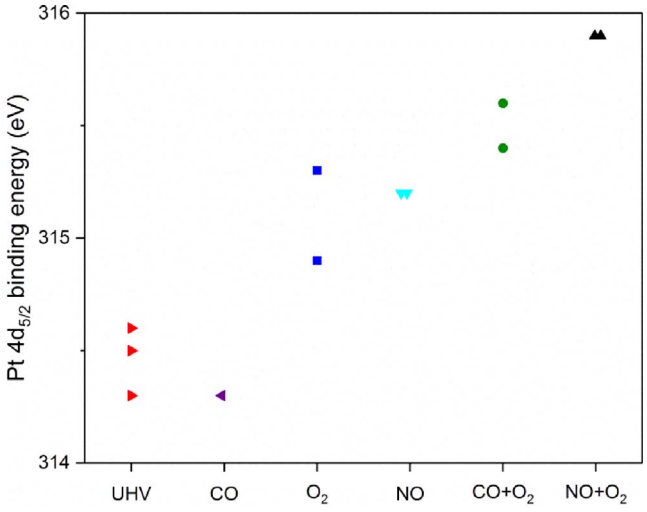

Fig. 4. The Pt $4d_{5/2}$ B.E. shift as a function of reaction atmosphere.

Some of the acquired Pt 4d peaks are shown in Fig. 5. Fig. 5A illustrates how large the shift in Pt 4d binding energy is in the NO + O_2 atmosphere, compared to vacuum. Fig. 5B illustrates that the shift in an NO-only atmosphere is smaller than the shift in the mixed NO + O_2 atmosphere. Finally, in Fig. 5C, the Pt 4d peak is compared between the UHV, CO + O_2, and NO + O_2 atmospheres, illustrating how the magnitude of the shift in Pt 4d binding energy increases as the atmosphere becomes increasingly oxidizing. Shifts in the O1s spectra under these conditions (not shown here) are consistent with the oxidation of Pt shown in the Pt 4d spectra, although definitive assignments can not be made because of the dominance of the spectrum by the O1s peak of Al_2O_3. Note that in the case of the mixed atmospheres, oxidation products (NO_2 and CO_2) were detected by the RGA, showing that a reaction was taking place on the catalyst surface as spectra were collected. Previous ex-situ studies have shown similar shifts in Pt photoelectron binding energies after pre-treatment with NO_2 [17], but here we show that such changes occur also during reaction between NO and O_2, where NO_2 is formed.

As shown in Table 1, under mixed atmospheres, the Pt $4d_{5/2}$ B.E. is not shifted significantly when the pressure ratio between components is changed from 1:1 to 1:100. As discussed above, the high Pt binding energies observed in the mixed NO + O_2 atmospheres were likely caused by oxidation of Pt by NO_2 formed in the reaction of NO with O_2 on the Pt surface. When the partial pressure of NO is much lower than that of O_2, only a relatively small amount of NO_2 (compared to O_2) is formed, yet the effect on the oxidation state of Pt can still be observed. In other words, we note that even at the low concentrations formed by an active catalyst, NO_2 has a strongly oxidizing effect on Pt, as shown previously by Ribeiro et al. [23]. Therefore, our results are applicable to an exhaust gas catalyst operating in a heavy-duty vehicle, where untreated exhaust typically has an NO:O_2 pressure ratio of around 1:100.

The aim of this study was to bridge not only the pressure gap

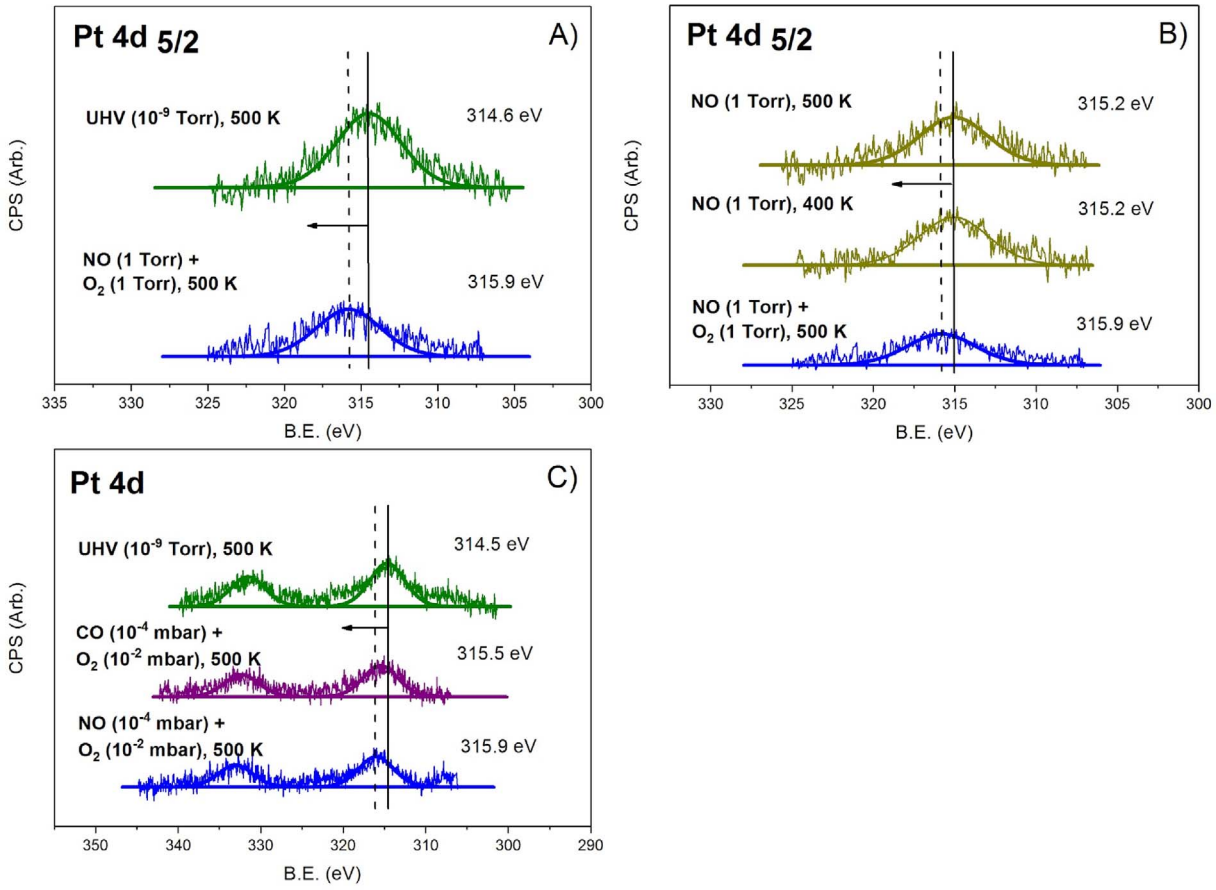

Fig. 5. A) The shift of Pt $4d_{5/2}$ under NO + O_2 as compared to UHV B) The increased oxidation of Pt under NO + O_2 as compared to NO. No temperature dependence of the Pt-shift can be observed C) Pt 4d shifts towards higher B.E. under both CO + O_2 and NO + O_2, with the latter being more pronounced.

between vacuum and operational pressures, but also the material gap between single crystal metal surfaces and supported porous catalysts. We have illustrated that experiments in a lab-based NAP-XPS system on supported porous catalysts can give mechanistic insights about the oxidation state of the catalytically active metal during reaction. In the future we will apply this method to study how the oxidation state of Pt during reaction is influenced by catalyst formulation. To study poisoning of the catalyst, we will investigate samples contaminated with Na, P and K. We also have underway XAS studies at the Singapore Synchrotron Light Source for these samples, the results of which will be correlated to NAP-XPS and STEM results.

4. Conclusions

We have illustrated that NAP-XPS can be used to probe the active catalytic surface of industrial-grade, porous catalysts (as opposed to single crystal model systems) used in vehicle exhaust after-treatment. The oxidation state of the catalytically active metal Pt was studied in different atmospheres modeling diesel exhaust conditions. The Pt 4d peak showed a significant shift to higher binding energies under oxidizing conditions, indicating that a surface oxide had been formed. The effect was especially pronounced under NO + O_2 atmospheres, likely due to deep oxidation of surface Pt caused by NO_2. Our in-situ NAP-XPS results are in line with previous ex-situ UHV studies after pretreatment by NO_2, and confirm the theory that the previously observed reverse temperature hysteresis in the NO oxidation reaction is due to oxidation of the platinum surface. Increased understanding of the mechanisms of such reversible catalyst deactivation can lead to optimization and increased efficiency of after-treatment systems, and by extension advances in meeting new emission standards.

Author contributions

The manuscript was written through contributions of all authors. All authors have given approval to the final version of the manuscript.

Conflict of interest

The authors declare no competing financial interests.

Acknowledgments

This work was partially supported by the National Science Foundation Division of Materials Research, grant NSF-DMR1506989. The Swedish Energy Agency is gratefully acknowledged for the financial support of the FFI project No 37178-1. Feng Tao acknowledges financial support from the Chemical Sciences, Geosciences and Biosciences Division, Office of Basic Energy Sciences, Office of Science, U.S. Department of Energy, under Grant No. DE-SC0014561, and U.S. National Science Foundation Career Award NSF-CHE-1462121.

References

[1] R.M. Heck, R.J. Farrauto, S.T. Gulati, Catalytic Air Pollution Control, Wiley Hoboken, NY, 2009.
[2] A. Russell, W.S. Epling, Diesel oxidation catalysts, Catal. Rev. 53 (2011) 337–423.
[3] M.K. Khair, A review of diesel particulate filter technologies, SAE Tech. Pap. Ser. (2003) 2003-01-2303-1-11.
[4] M. Koebel, M. Elsener, M. Kleemann, Urea-SCR: a promising technique to reduce NO_x emissions from automotive diesel engines, Catal. Today 59 (2000) 335–346.
[5] F. Tao, S. Dag, L.-W. Wang, Z. Liu, D.R. Butcher, H. Bluhm, M. Salmeron, G.A. Somorjai, Break-up of stepped platinum catalyst surfaces by high CO coverage, Science 327 (2010) 850–853.
[6] P.L. Hansen, J.B. Wagner, S. Helveg, J.R. Rostrup-Nielsen, B.S. Clausen, H. Topsøe,

Atom-resolved imaging of dynamic shape changes in supported copper nanocrystals, Science 295 (2002) 2053–2055.
[7] F. Tao, Design of an in-house ambient pressure AP-XPS using a bench-top X-ray source and the surface chemistry of ceria under reaction conditions, Chem. Commun. 48 (2012) 3812–3814.
[8] D.F. Ogletree, H. Bluhm, G. Lebedev, C.S. Fadley, Z. Hussain, M.A. Salmeron, Differentially pumped electrostatic lens system for photoemission studies in the millibar range, Rev. Sci. Instrum. 73 (2002) 3872–3877.
[9] M.E. Grass, P.G. Karlsson, F. Aksoy, M. Lundqvist, B. Wannberg, B.S. Mun, Z. Hussain, Z. Liu, New ambient pressure photoemission endstation at Advanced Light Source beamline 9.3.2, Rev. Sci. Instrum. 81 (2010) 053106-1-7.
[10] M. Salmeron, R. Schlögl, Ambient pressure photoelectron spectroscopy: a new tool for surface science and nanotechnology, Surf. Sci. Rep. 63 (2008) 169–199.
[11] D.R. Butcher, M.E. Grass, Z. Zeng, F. Aksoy, H. Bluhm, W.-X. Li, B.S. Mun, G.A. Somorjai, Z. Liu, In situ oxidation study of Pt(110) and its interaction with CO, J. Am. Chem. Soc. 133 (2011) 20319–20325.
[12] R. Toyoshima, M. Yoshida, Y. Monya, K. Suzuki, K. Amemiya, K. Mase, B.S. Mun, H. Kondoh, In situ photoemission observation of catalytic CO oxidation reaction on Pd(110) under near-ambient pressure conditions: evidence for the Langmuir-Hinshelwood mechanism, J. Phys. Chem. C 117 (2013) 20617–20624.
[13] R. Toyoshima, M. Yoshida, Y. Monya, K. Suzuki, B.S. Mun, K. Amemiya, K. Mase, H. Kondoh, Active surface oxygen for catalytic CO oxidation on Pd(100) proceeding under near ambient pressure conditions, J. Phys. Chem. Lett. 3 (2012) 3182–3187.
[14] R. Toyoshima, M. Yoshida, Y. Monya, Y. Kousa, K. Suzuki, H. Abe, B.S. Mun, K. Mase, K. Amemiya, H. Kondoh, In situ ambient pressure XPS study of CO oxidation reaction on Pd(111) surfaces, J. Phys. Chem. C 116 (2012) 18691–18697.
[15] W. Hauptmann, M. Votsmeier, J. Gieshoff, A. Drochner, H. Vogel, Inverse hysteresis during the NO oxidation on Pt under lean conditions, Appl. Catal. B 93 (2009) 22–29.
[16] L. Olsson, E. Fridell, The influence of pt oxide formation and pt dispersion on the reactions $NO_2 \Leftrightarrow NO + 1/2\ O_2$ over Pt/Al_2O_3 and $Pt/BaO/Al_2O_3$, J. Catal. 210 (2002) 340–353.
[17] J. Després, M. Elsener, M. Koebel, O. Kröcher, B. Schnyder, A. Wokaun, Catalytic oxidation of nitrogen monoxide over Pt/SiO_2, Appl. Catal. B 50 (2004) 73–82.
[18] R.B. Getman, W.F. Schneider, A.D. Smeltz, W.N. Delgass, F.H. Ribeiro, Oxygen-coverage effects on molecular dissociations at a Pt metal surface, Phys. Rev. Lett. 102 (2009) 076101-1-3.
[19] A. Boubnov, S. Dahl, E. Johnson, A.P. Molina, S.B. Simonsen, F.M. Cano, S. Helveg, L.J. Lemus-Yegres, J.-D. Grunwaldt, Structure–activity relationships of Pt/Al_2O_3 catalysts for CO and NO oxidation at diesel exhaust conditions, Appl. Catal. B 126 (2012) 315–325.
[20] J.-Y. Chung, F. Aksoy, M.E. Grass, H. Kondoh, P. Ross Jr., Z. Liu, M.S. Mun, In-situ study of the catalytic oxidation of CO on a Pt(110) surface using ambient pressure X-ray photoelectron spectroscopy, Surf. Sci. 603 (2009) L35–L38.
[21] A. Manasilp, E. Gulari, Selective CO oxidation over Pt/alumina catalysts for fuel cell applications, Appl. Catal. B 37 (2002) 17–25.
[22] K. Hauff, U. Tuttlies, G. Eigenberger, U. Nieken, Platinum oxide formation and reduction during NO oxidation on a diesel oxidation catalyst-experimental results, Appl. Catal. B 123–124 (2012) 107–116.
[23] S.S. Mulla, N. Chen, L. Cumaranatunge, G.E. Blau, D.Y. Zemlyanov, W.N. Delgass, W.S. Epling, F.H. Ribeiro, Reaction of NO and O_2 to NO_2 on Pt: kinetics and catalyst deactivation, J. Catal. 241 (2006) 389–399.
[24] R. Khazanchi, D. Reddy, D. Bhatia, Kinetic model for the reversible deactivation of a Pt/Al_2O_3 catalyst during NO oxidation, Chem. Eng. J. 314 (2017) 139–151.
[25] D. Bhatia, R.W. McCabe, M.P. Harold, V. Balakotaiah, Experimental and kinetic study of NO oxidation on model Pt catalysts, J. Catal. 266 (2009) 106–119.
[26] L. Nguyen, F. Tao, Development of a reaction cell for in-situ/operando studies of surface of a catalyst under a reaction condition and during catalysis, Rev. Sci. Instrum. 87 (2016) 064101-1-4.
[27] D.E. Jesson, S.J. Pennycook, Incoherent imaging of crystals using thermally scattered electrons, Proc. R. Soc. Lond. Ser. A 449 (1995) 273–293.
[28] C.H. Bartholomew, R.J. Farrauto, Fundamentals of Industrial Catalytic Processes, Wiley, Hoboken, NJ, 2005 pp 60–117 (Chapter 2).
[29] G. Ertl, Reactions at surfaces: from atoms to complexity (Nobel lecture), Angew. Chem. Intl. Ed. 47 (2008) 3524–3535.